Camouflaged Object Segmentation with Distraction Mining (Supplementary Material)

Haiyang Mei[1] Ge-Peng Ji[2,4] Ziqi Wei[3,⋆] Xin Yang[1,⋆] Xiaopeng Wei[1] Deng-Ping Fan[4]
[1] Dalian University of Technology [2] Wuhan University [3] Tsinghua University [4] IIAI
https://mhaiyang.github.io/CVPR2021_PFNet/index

1. Additional Results

To further demonstrate the superiority of our method, in this supplementary, we present the quantitative comparison results on the four super-classes of the COD10K dataset [3] in Table 1 and show more qualitative comparison results in Figure 1, 2, 3, 4, 5, 6, 7, 8, 9, and 10.

Compared Methods. We compare our PFNet against 18 strong, state-of-the-art baselines: object detection method FPN [8]; semantic segmentation method PSPNet [14]; instance segmentation methods Mask RCNN [5], HTC [1], and MSRCNN [7]; shadow detection methods DSC [6] and BDRAR [18]; medical image segmentation methods UNet++ [17] and PraNet [4]; salient object detection methods PiCANet [9], BASNet [11], CPD [13], PFANet [16], EGNet [15], F3Net [12], GCPANet [2], and MINet-R [10]; and camouflaged object segmentation method SINet [3]. For a fair comparison, all the prediction maps of the above methods are either provided by the public website or produced by running the models retrained with open source codes. Besides, all the prediction maps are evaluated with the same code.

⋆ Xin Yang (xinyang@dlut.edu.cn) and Ziqi Wei are the corresponding authors.

Methods	Pub.'Year	*COD10K*-Aquatic 474 images				*COD10K*-Terrestrial 699 images				*COD10K*-Flying 714 images				*COD10K*-Amphibian 124 images			
		$S_\alpha\uparrow$	$E_\phi^{ad}\uparrow$	$F_\beta^w\uparrow$	$M\downarrow$	$S_\alpha\uparrow$	$E_\phi^{ad}\uparrow$	$F_\beta^w\uparrow$	$M\downarrow$	$S_\alpha\uparrow$	$E_\phi^{ad}\uparrow$	$F_\beta^w\uparrow$	$M\downarrow$	$S_\alpha\uparrow$	$E_\phi^{ad}\uparrow$	$F_\beta^w\uparrow$	$M\downarrow$
FPN$^\circ$ [8]	CVPR'17	.684	.729	.432	.103	.668	.675	.353	.071	.726	.724	.440	.061	.744	.772	.497	.065
PSPNet$^\bullet$ [14]	CVPR'17	.659	.706	.396	.111	.658	.652	.332	.074	.700	.703	.394	.067	.736	.739	.463	.072
Mask RCNN* [5]	ICCV'17	.560	.721	.344	.123	.608	.749	.380	.070	.644	.767	.449	.063	.665	.784	.487	.081
UNet++§ [17]	DLMIA'17	.599	.708	.347	.121	.593	.692	.288	.081	.659	.745	.397	.068	.677	.754	.434	.079
DSC$^\triangle$ [6]	CVPR'18	.746	.799	.563	.074	.724	.755	.474	.051	.791	.807	.581	.040	.812	.834	.636	.042
PiCANet† [9]	CVPR'18	.629	.698	.335	.120	.625	.640	.273	.084	.677	.696	.347	.076	.704	.727	.405	.086
BDRAR$^\triangle$ [18]	ECCV'18	.739	.819	.595	.071	.727	.818	.540	.050	.780	.860	.627	.039	.802	.869	.667	.046
HTC* [1]	CVPR'19	.507	.495	.183	.129	.530	.485	.170	.078	.582	.559	.274	.070	.606	.598	.331	.088
MSRCNN* [7]	CVPR'19	.614	.686	.397	.107	.611	.672	.361	.070	.674	.744	.466	.058	.722	.786	.555	.055
BASNet† [11]	CVPR'19	.620	.678	.374	.134	.601	.630	.301	.109	.664	.711	.403	.086	.708	.739	.477	.087
CPD† [13]	CVPR'19	.739	.777	.529	.082	.714	.730	.445	.058	.777	.781	.543	.046	.794	.805	.587	.051
PFANet† [16]	CVPR'19	.629	.647	.319	.162	.609	.577	.237	.123	.657	.632	.299	.113	.690	.672	.358	.119
EGNet† [15]	ICCV'19	.725	.784	.528	.080	.704	.748	.445	.054	.768	.794	.543	.044	.788	.833	.606	.048
F3Net† [12]	AAAI'20	.772	.824	.620	.069	.760	.810	.566	.045	.815	.857	.657	.034	.824	.860	.680	.042
GCPANet† [2]	AAAI'20	.784	.817	.617	.063	.763	.760	.527	.045	.815	.821	.623	.034	.843	.844	.679	.037
PraNet§ [4]	MICCAI'20	.781	.832	.643	.065	.756	.810	.565	.046	.819	.864	.669	.033	.842	.892	.717	.035
MINet-R† [10]	CVPR'20	.752	.832	.595	.066	.723	.806	.513	.044	.790	.851	.622	.034	.808	.881	.662	.035
SINet* [3]	CVPR'20	.758	.806	.570	.073	.743	.765	.491	.050	.798	.816	.580	.040	.827	.847	.654	.042
PFNet*	Ours	**.793**	**.865**	**.675**	**.055**	**.773**	**.850**	**.606**	**.040**	**.824**	**.887**	**.691**	**.030**	**.848**	**.896**	**.740**	**.031**

Table 1. Comparison of the proposed method against 18 state-of-the-art methods in the relevant fields on four super-classes of the COD10K dataset [3] in terms of the structure-measure S_α (larger is better), the adaptive E-measure E_ϕ^{ad} (larger is better), the weighted F-measure F_β^w (larger is better), and the mean absolute error M (smaller is better). All the prediction maps are evaluated with the same code. The best results are marked in **bold**. $\circ$: object detection method. $\bullet$: semantic segmentation method. $\star$: instance segmentation methods. $\triangle$: shadow detection methods. §: medical image segmentation methods. †: SOD methods. *: COS methods. Our method outperforms other counterparts with a large margin under all four standard evaluation metrics on all four super-classes of the COD10K dataset [3].

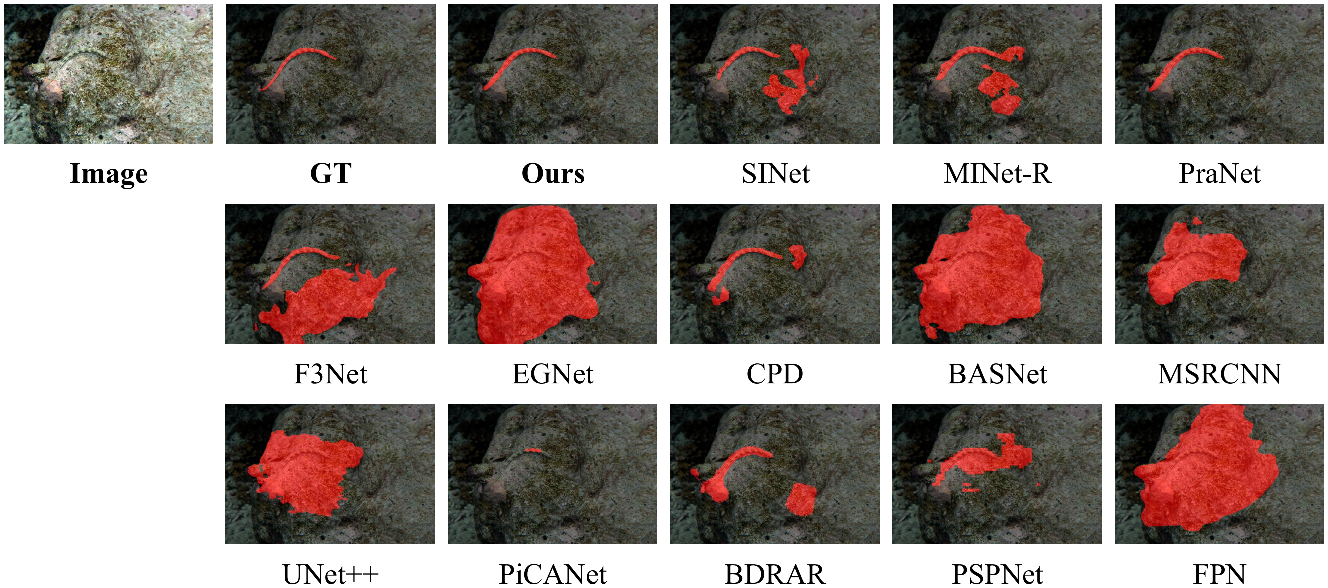

Figure 1. Visual comparison of our proposed PFNet with state-of-the-art methods on image *COD10K-CAM-1-Aquatic-13-Pipefish-841.jpg*.

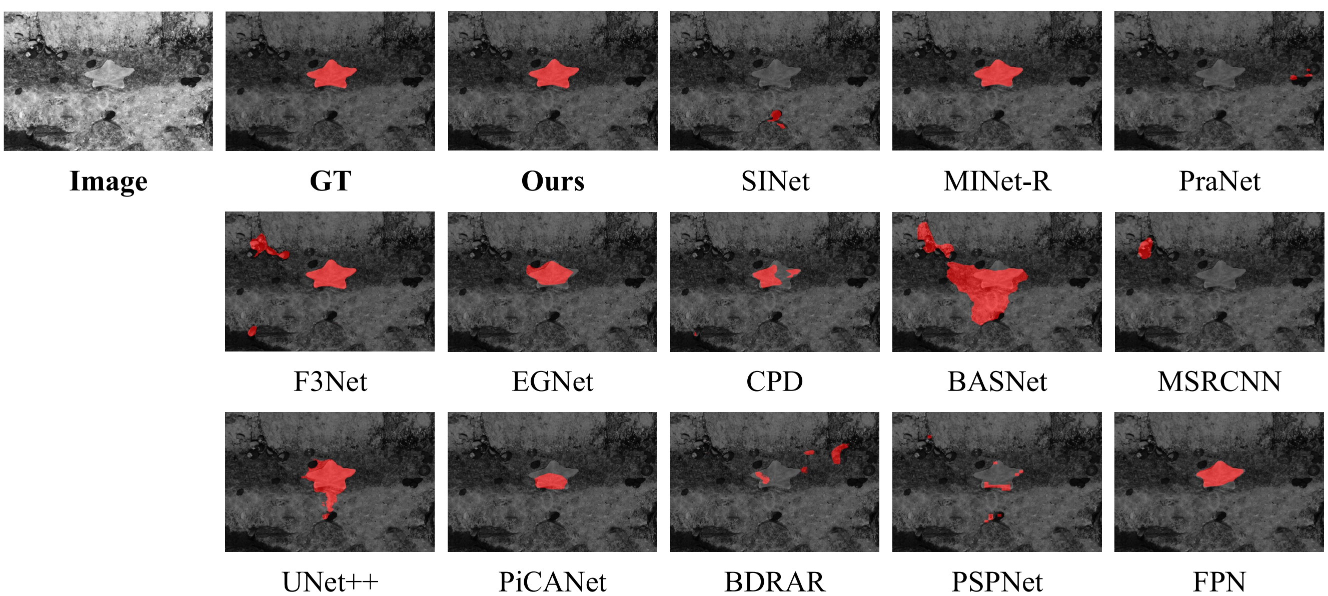

Figure 2. Visual comparison of our proposed PFNet with state-of-the-art methods on image *COD10K-CAM-1-Aquatic-18-StarFish-1171.jpg*.

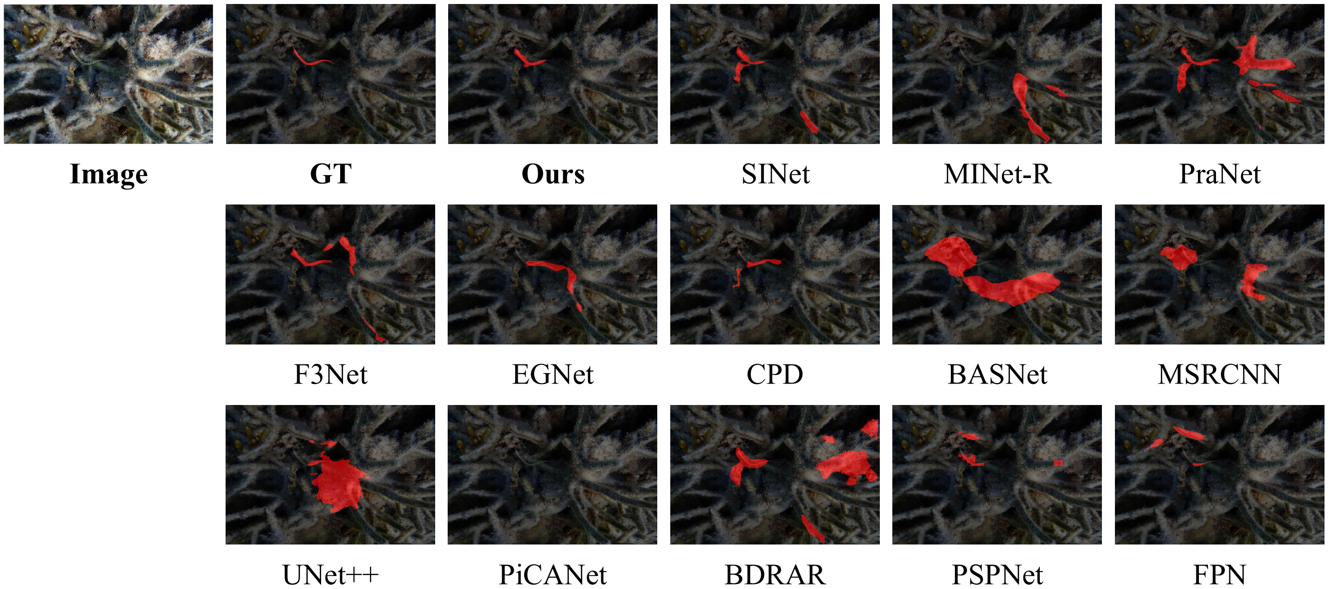

Figure 3. Visual comparison of our proposed PFNet with state-of-the-art methods on image *COD10K-CAM-1-Aquatic-13-Pipefish-614.jpg*.

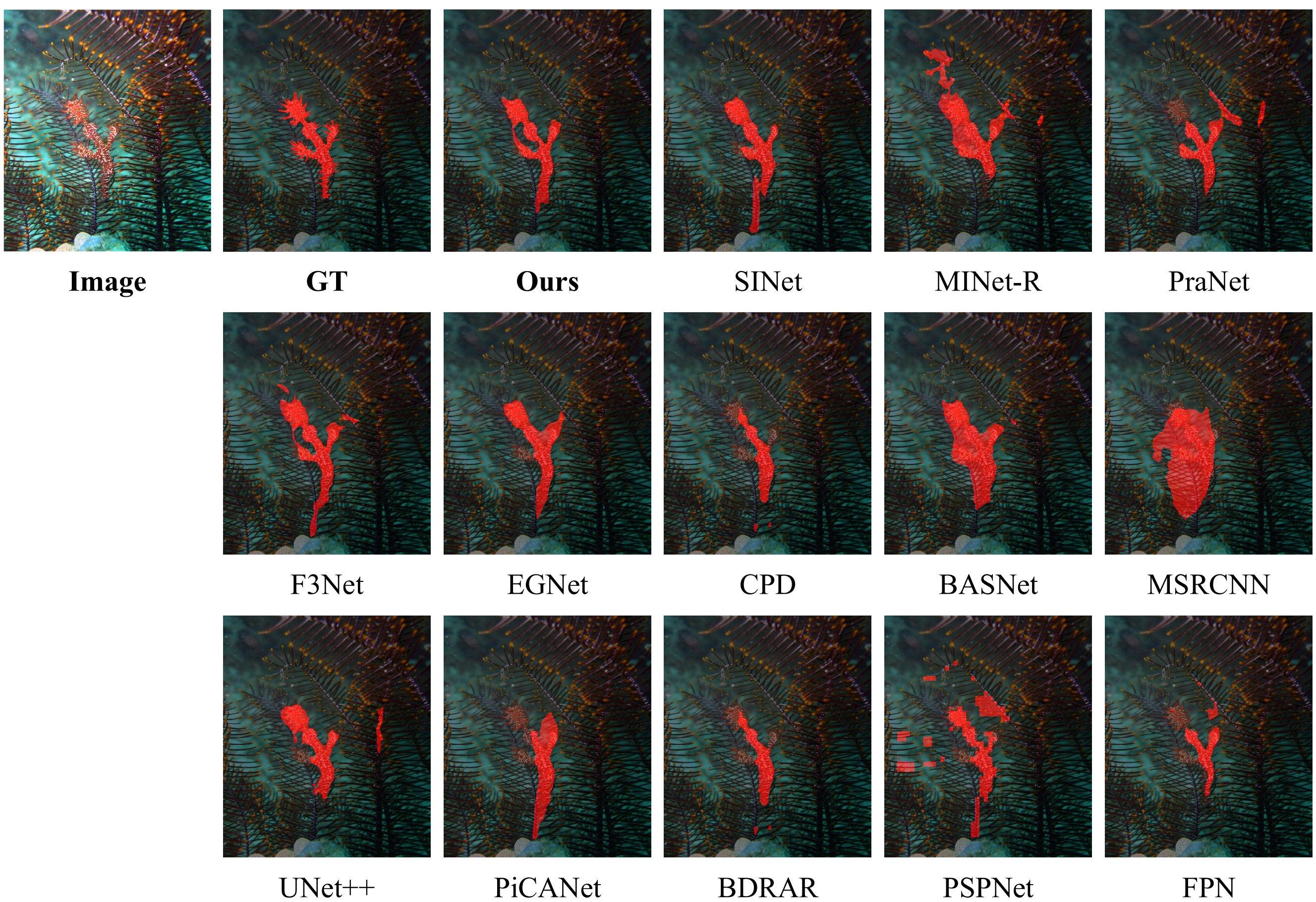

Figure 4. Visual comparison of our proposed PFNet with state-of-the-art methods on image *COD10K-CAM-1-Aquatic-9-GhostPipefish-333.jpg*.

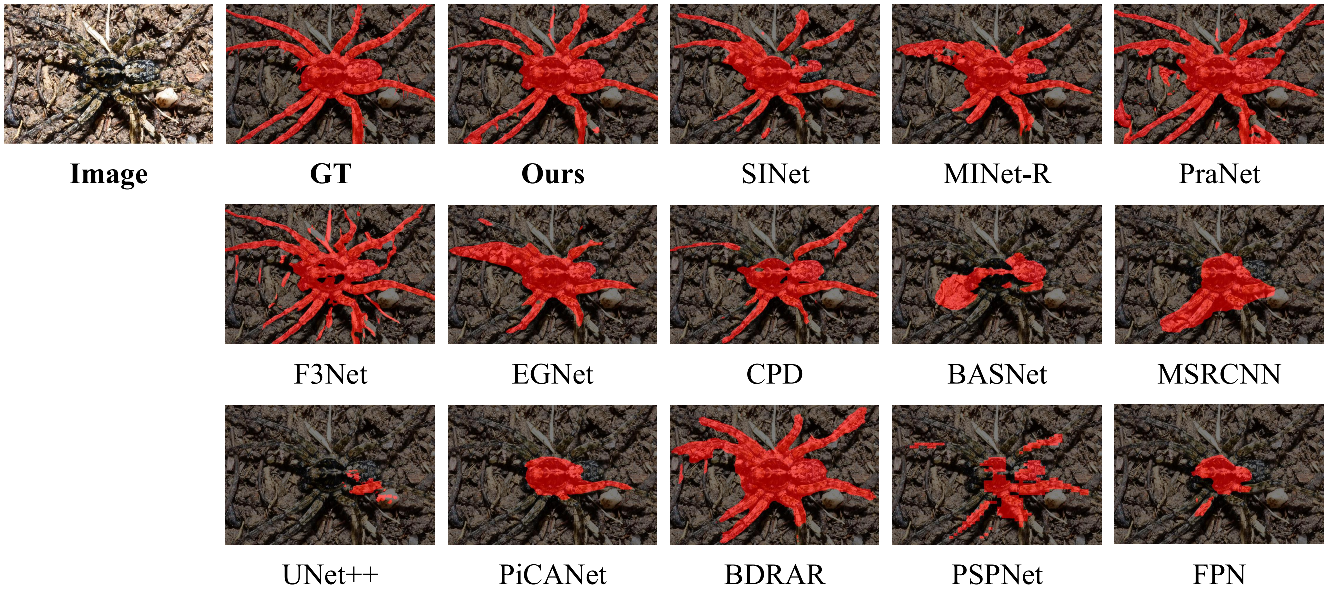

Figure 5. Visual comparison of our proposed PFNet with state-of-the-art methods on image *COD10K-CAM-2-Terrestrial-45-Spider-2649.jpg*.

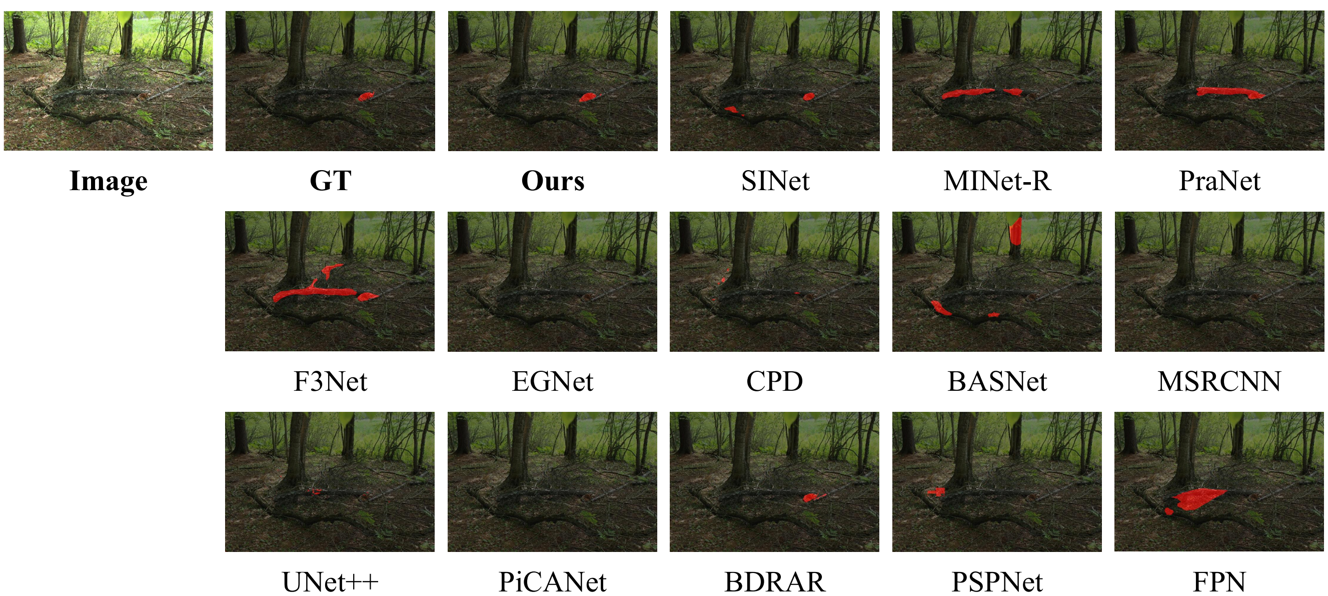

Figure 6. Visual comparison of our proposed PFNet with state-of-the-art methods on image *COD10K-CAM-2-Terrestrial-28-Deer-1790.jpg*.

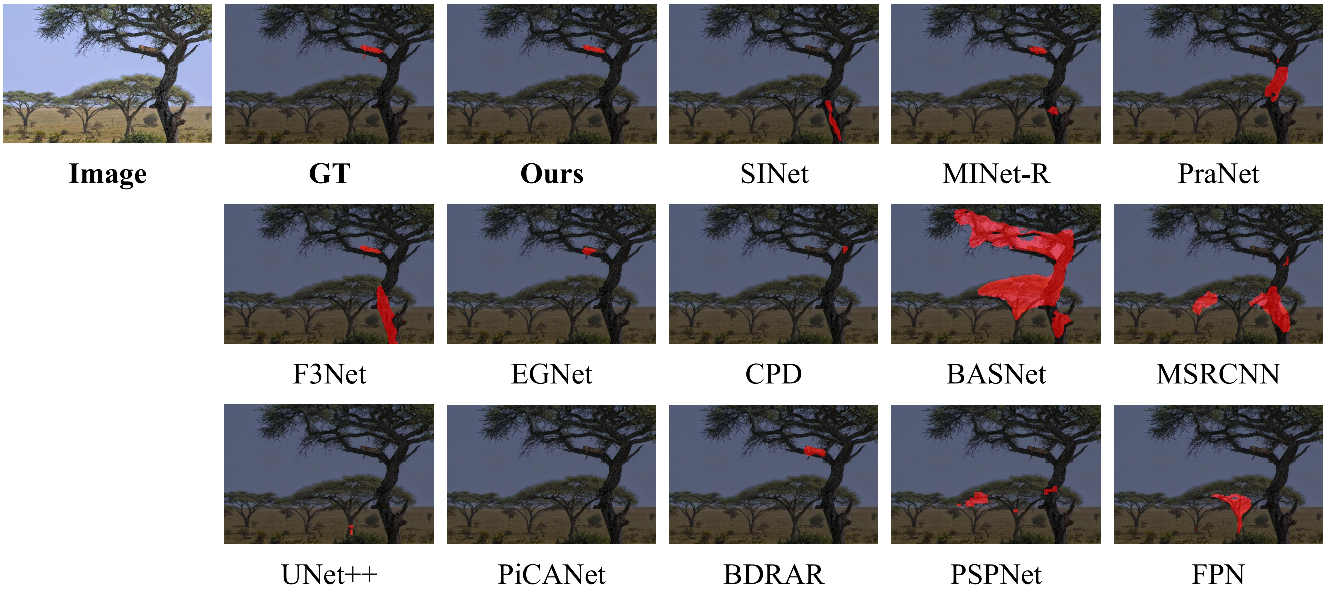

Figure 7. Visual comparison of our proposed PFNet with state-of-the-art methods on image *COD10K-CAM-2-Terrestrial-36-Leopard-2071.jpg*.

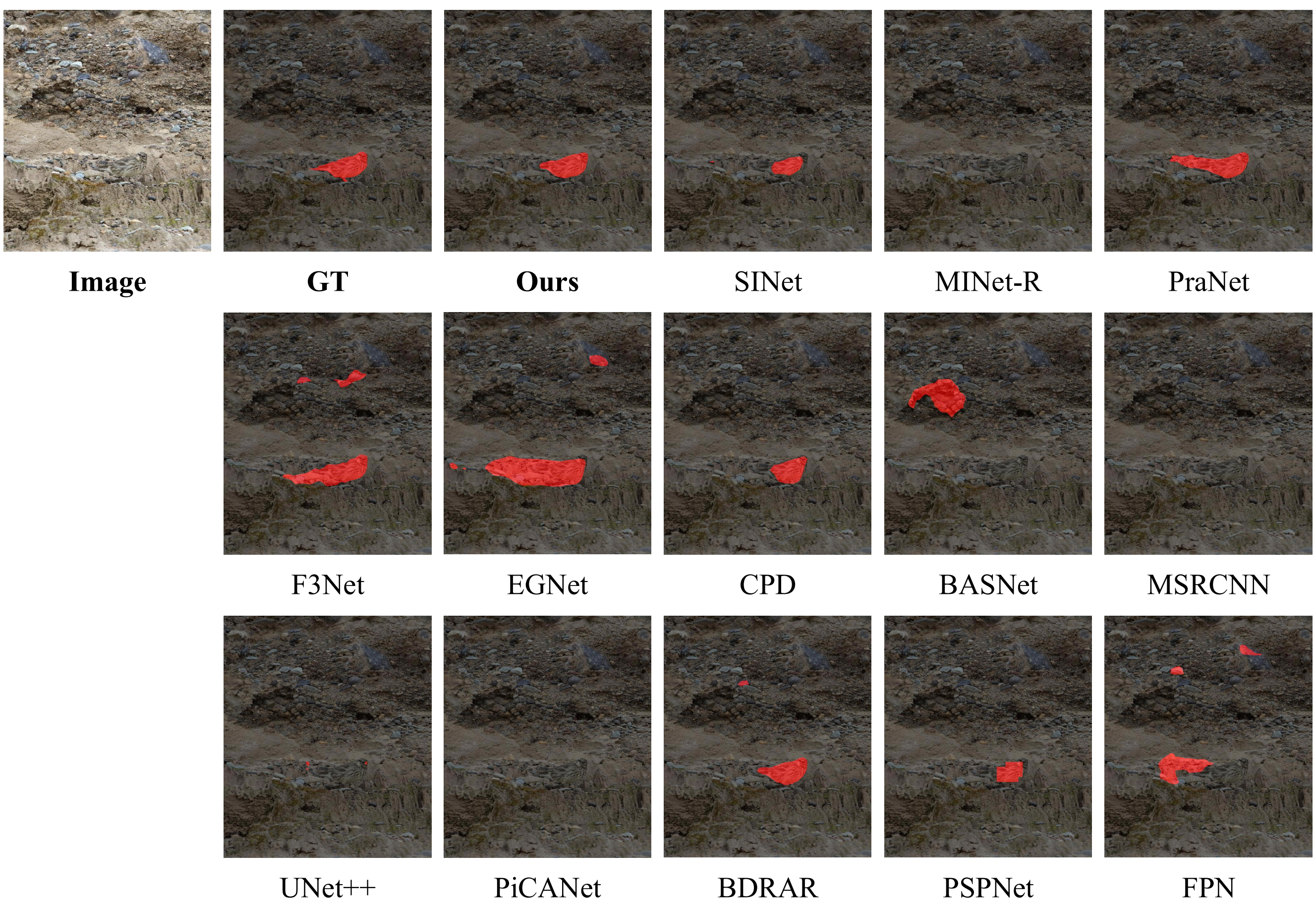

Figure 8. Visual comparison of our proposed PFNet with state-of-the-art methods on image *COD10K-CAM-3-Flying-53-Bird-3155.jpg*.

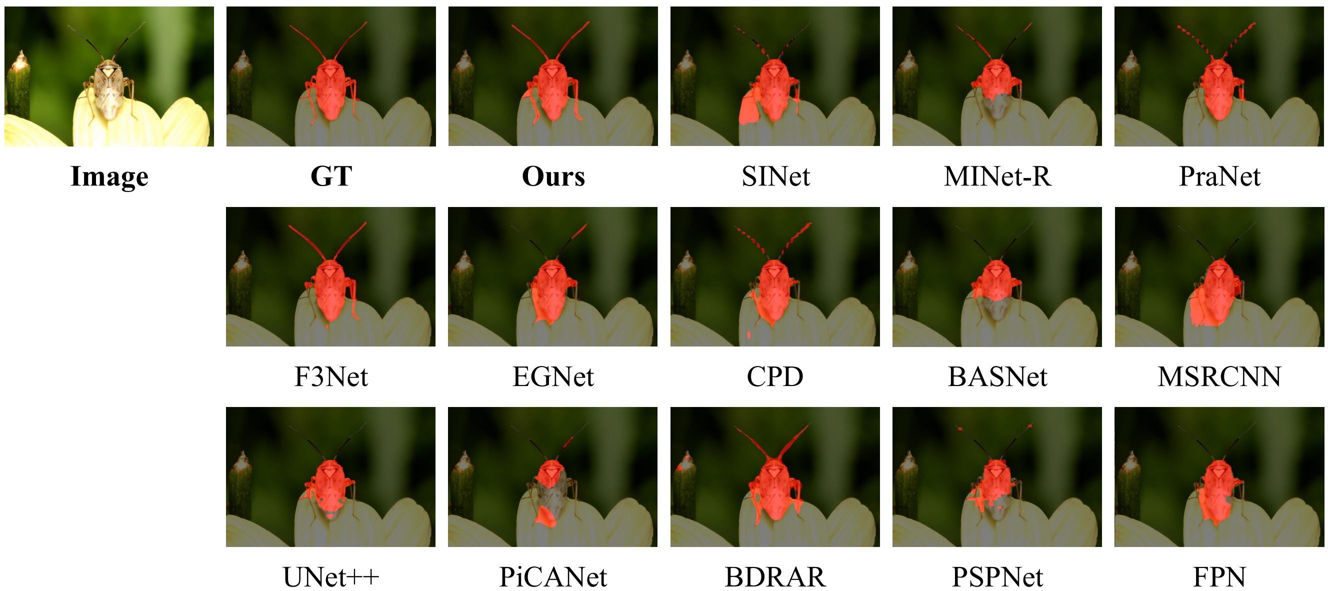

Figure 9. Visual comparison of our proposed PFNet with state-of-the-art methods on image *COD10K-CAM-2-Terrestrial-22-Bug-1286.jpg*.

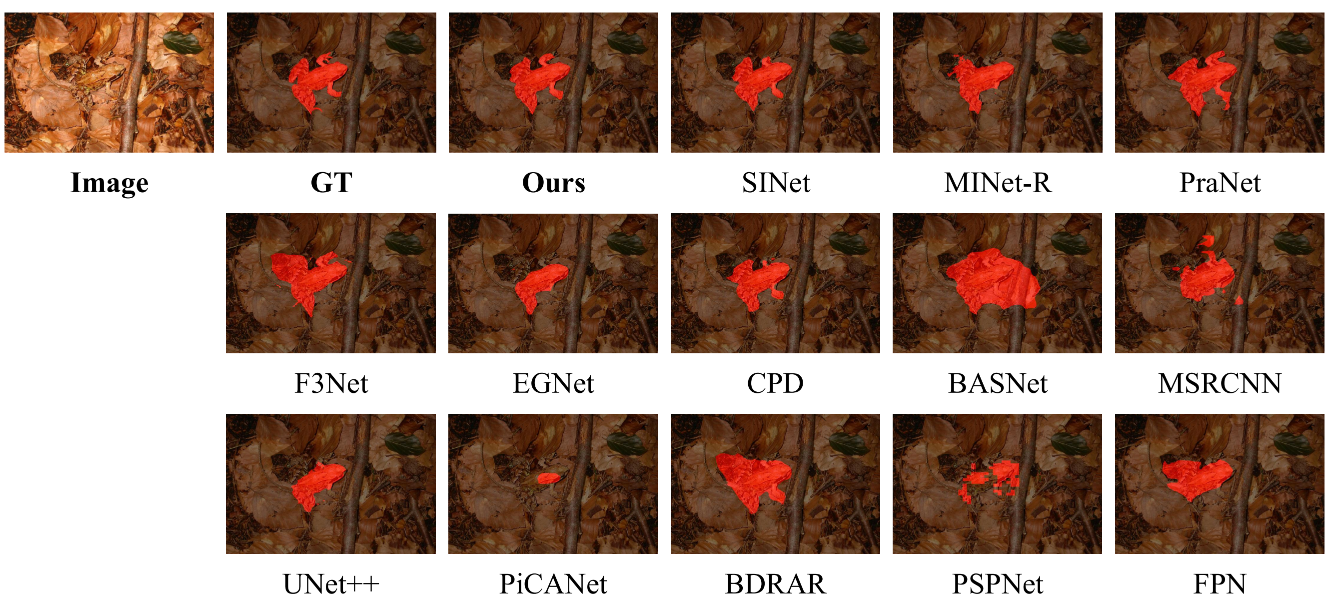

Figure 10. Visual comparison of our proposed PFNet with state-of-the-art methods on image *animal-67.jpg*.

References

[1] Kai Chen, Jiangmiao Pang, Jiaqi Wang, Yu Xiong, Xiaoxiao Li, Shuyang Sun, Wansen Feng, Ziwei Liu, Jianping Shi, Wanli Ouyang, et al. Hybrid task cascade for instance segmentation. In *CVPR*, 2019. 1, 2

[2] Zuyao Chen, Qianqian Xu, Runmin Cong, and Qingming Huang. Global context-aware progressive aggregation network for salient object detection. In *AAAI*, 2020. 1, 2

[3] Deng-Ping Fan, Ge-Peng Ji, Guolei Sun, Ming-Ming Cheng, Jianbing Shen, and Ling Shao. Camouflaged object detection. In *CVPR*, 2020. 1, 2

[4] Deng-Ping Fan, Ge-Peng Ji, Tao Zhou, Geng Chen, Huazhu Fu, Jianbing Shen, and Ling Shao. Pranet: Parallel reverse attention network for polyp segmentation. In *MICCAI*, 2020. 1, 2

[5] Kaiming He, Georgia Gkioxari, Piotr Dollár, and Ross Girshick. Mask r-cnn. In *ICCV*, 2017. 1, 2

[6] Xiaowei Hu, Lei Zhu, Chi-Wing Fu, Jing Qin, and Pheng-Ann Heng. Direction-aware spatial context features for shadow detection. In *CVPR*, 2018. 1, 2

[7] Zhaojin Huang, Lichao Huang, Yongchao Gong, Chang Huang, and Xinggang Wang. Mask scoring r-cnn. In *CVPR*, 2019. 1, 2

[8] Tsung-Yi Lin, Piotr Dollár, Ross Girshick, Kaiming He, Bharath Hariharan, and Serge Belongie. Feature pyramid networks for object detection. In *CVPR*, 2017. 1, 2

[9] Nian Liu, Junwei Han, and Ming-Hsuan Yang. Picanet: Learning pixel-wise contextual attention for saliency detection. In *CVPR*, 2018. 1, 2

[10] Youwei Pang, Xiaoqi Zhao, Lihe Zhang, and Huchuan Lu. Multi-scale interactive network for salient object detection. In *CVPR*, 2020. 1, 2

[11] Xuebin Qin, Zichen Zhang, Chenyang Huang, Chao Gao, Masood Dehghan, and Martin Jagersand. Basnet: Boundary-aware salient object detection. In *CVPR*, 2019. 1, 2

[12] Jun Wei, Shuhui Wang, and Qingming Huang. F3net: Fusion, feedback and focus for salient object detection. In *AAAI*, 2020. 1, 2

[13] Zhe Wu, Li Su, and Qingming Huang. Cascaded partial decoder for fast and accurate salient object detection. In *CVPR*, 2019. 1, 2

[14] Hengshuang Zhao, Jianping Shi, Xiaojuan Qi, Xiaogang Wang, and Jiaya Jia. Pyramid scene parsing network. In *CVPR*, 2017. 1, 2

[15] Jia-Xing Zhao, Jiang-Jiang Liu, Deng-Ping Fan, Yang Cao, Jufeng Yang, and Ming-Ming Cheng. Egnet: Edge guidance network for salient object detection. In *ICCV*, 2019. 1, 2

[16] Ting Zhao and Xiangqian Wu. Pyramid feature attention network for saliency detection. In *CVPR*, 2019. 1, 2

[17] Zongwei Zhou, Mahfuzur Rahman Siddiquee, Nima Tajbakhsh, and Jianming Liang. Unet++: A nested u-net architecture for medical image segmentation. *DLMIA*, 2018. 1, 2

[18] Lei Zhu, Zijun Deng, Xiaowei Hu, Chi-Wing Fu, Xuemiao Xu, Jing Qin, and Pheng-Ann Heng. Bidirectional feature pyramid network with recurrent attention residual modules for shadow detection. In *ECCV*, 2018. 1, 2